Hydrological Sciences Journal

ISSN: (Print) (Online) Journal homepage: https://www.tandfonline.com/loi/thsj20

A reverse engineering approach across small hydropower plants: a hidden treasure of hydrological data?

Georgia-Konstantina Sakki, Ioannis Tsoukalas & Andreas Efstratiadis

To cite this article: Georgia-Konstantina Sakki, Ioannis Tsoukalas & Andreas Efstratiadis (2021): A reverse engineering approach across small hydropower plants: a hidden treasure of hydrological data?, Hydrological Sciences Journal, DOI: 10.1080/02626667.2021.2000992

To link to this article: https://doi.org/10.1080/02626667.2021.2000992

Accepted author version posted online: 01 Nov 2021.

Publisher: Taylor & Francis & IAHS

Journal: *Hydrological Sciences Journal*

DOI: 10.1080/02626667.2021.2000992

A reverse engineering approach across small hydropower plants: a hidden treasure of hydrological data?

Georgia-Konstantina Sakki*[a], Ioannis Tsoukalas[a], Andreas Efstratiadis[a]

[a]Department of Water Resources and Environmental Engineering, School of Civil Engineering, National Technical University of Athens, Heroon Polytechneiou 5, 15780 Zographou, Greece

*Correspondence: andreas@itia.ntua.gr

Abstract

The limited availability of hydrometric data makes the design, management, and real-time operation of water systems a difficult task. Here, we propose a generic stochastic framework for the so-called inverse problem of hydroelectricity, using energy production data from small hydropower plants (SHPPs) to retrieve the upstream inflows. In this context, we investigate the alternative configurations of water-energy transformations across SHPPs of negligible storage capacity, which are subject to multiple uncertainties. We focus on two key sources, i.e. observational errors in energy production and uncertain efficiency curves of turbines. In order to extract the full hydrograph, we also extrapolate the high and low flows outside of the range of operation of turbines, by employing empirical rules for representing the rising and falling limbs of the simulated hydrographs. This framework is demonstrated to a real-world system at Evinos river basin, Greece. By taking advantage of the proposed methodology, SHPPs may act as potential hydrometric stations and improve the existing information in poorly gauged areas.

Keywords: renewable energy; hydropower; run-of-river plants; uncertainty; simulation; efficiency curves

1 Introduction

All hydro-environmental sciences and associated technologies (e.g., hydrology, ecology, hydrometeorology, hydroclimatology, hydropower technology, agricultural technology, etc.) are founded upon flow observations. In particular, historical data provide the irreplaceable means for understanding and modelling the long-term behavior of water resource systems and assess their uncertainties, while real-time data are essential for assessing their current status and making short-term predictions about the water availability and the associated risks.

However, it is generally recognized that the actual status of hydrometric data worldwide is still not satisfactory, particularly in developing countries (Blöschl *et al.*, 2019, Dixon *et al.*, 2020, Viglione *et al.*, 2010) while there is also a global threat to the maintenance of existing monitoring infrastructures, mainly due to funding and political pressures (Fekete *et al.*, 2015, Hannah *et al.*, 2011). Even in the EU, in many places the availability of hydrometric data is rather limited, in terms of desirable spatial density, temporal resolution and time extent. To address this problem, many efforts are put on technological innovations, such as remote sensing applications (Kittel *et al.*, 2021) and citizen engagement via crowdsourced data (Avellaneda *et al.*, 2020), yet both providing only approximative or macroscopic hydrological information.

Here, we manifest an alternative data source, offered by small hydropower plants (SHPPs) without storage capacity or any other upstream regulation. Our emphasis is put to the so-called run-of-river plants, that divert part of the river flow through an intake structure, which is next released to the turbine station from a large elevation difference (for this reason, this category of SHPPs is also referred to as high-head). These are generally developed in small rivers or tributaries at mountainous catchments, where the available hydrometric information is often very limited, despite the improvements made in some areas for enhancing ground-based measurements, e.g., through wireless sensor networks (Avanzi *et al.*, 2020, Kerkez *et al.*, 2012). The operation of these works differs significantly from hydroelectric reservoirs, since they do not offer regulation of flows, thus the energy production is a direct conversion of the actual inflow. Following this, the inflow is also a conversion of energy, which is an easily measurable quantity. In this context, SHPPs may be also encountered as hydrometric stations, by solving the underlying *inverse problem of hydroelectricity*.

To our knowledge, reverse engineering approaches in hydroelectric works have been formulated so far as the estimation of actual efficiency on the basis of power production data. For instance, Hidalgo et al. (2012) have proposed an elegant methodology to retrieve the flow passing through the penstock and next adjust the efficiency function for each generating unit, which is yet only applicable for large hydroelectric reservoirs, based on water elevation measurements, upstream (i.e., the reservoir) and downstream (in the tailrace). Regarding the inflows to hydroelectric reservoirs, these are estimated in a much simpler manner, namely on the basis of water balance data (e.g., A. Efstratiadis *et al.*, 2014).

However, in the case of SHPPs without storage capacity, reverse engineering approaches for streamflow estimations based on energy production data are not straightforward, due to two reasons. The first is the nonlinearity of the flow-energy transformation. One the one hand, the net head and efficiency, which are embedded in the energy production formula, are nonlinear functions of discharge. On the other hand, SHPPs operate only within a specific flow range [q_{min}, q_{max}], determined by the power capacity, P_{max}, and the type of turbines, that make the problem ill-posed. Besides the inherent uncertainty induced by the aforementioned complexities, there are further sources of uncertainty that refer to the internal processes (i.e., representation of hydraulic and energy losses) and the measurement of produced electric power, as well.

This research aims at developing a stochastic framework for retrieving streamflow time series at a given SHPP site, on the basis of uncertain power data and/or uncertain efficiency. The problem is posed differently for the three flow conditions, i.e. above, below and within the range of turbine operation. We remark that if the power production is zero, then we do know that the streamflow is either below the minimum discharge of turbines, q_{min}, or above a quite large safety value, q_s, while if the power capacity is produced, we know that the streamflow exceeds the nominal discharge, q_{max}; in all these cases, the exact value of the incoming streamflow is unknown. In this respect, we first define the three configurations of the associated flow-energy conversion problem, which follows the organization of the article, i.e.:

- Forward configuration, i.e. assessment of the energy produced for given inflow data and known technical characteristics.
- Inverse configuration by means of reverse engineering, i.e. estimation of the discharge by using energy production data and known technical characteristics.
- Derivation of unknown technical characteristics (handled as parameters) through calibration, based on known energy and flow data.

An important issue of our methodological framework is the estimation of efficiency, for which we provide a novel analytical expression that replaces the old-fashioned efficiency nomographs to facilitate computations and parameterize the associated uncertainties. The methodology of extracting inflows from energy data is tested in a SHPP under study in Greece, by solving the inverse problem under varying sources of uncertainty.

2 The forward problem

2.1 Problem formulation

Let consider a run-of-river plant of negligible storage capacity and without any regulation facility upstream. In the generic case, this comprises two turbines of power capacity, P_1 and P_2, operating within flow ranges ($q_{1,min}, q_{1,max}$) and ($q_{2,min}, q_{2,max}$), respectively. Typically, P_1 and P_2 are quite different, to ensure an optimal exploitation of the available inflows, since the total flow range of the system fluctuates from the minimum value between ($q_{1,min}, q_{2,min}$) and the sum $q_{1,max} + q_{2,max}$ (Anagnostopoulos & Papantonis, 2007). The maximum discharge of each turbine is determined by its power capacity:

$$q_{i,max} = \frac{P_i}{\gamma\, \eta_{i,max}\, h_n} \tag{1}$$

where $\eta_{i,max}$ is the total efficiency, which depends on the turbine type, γ = 9.81 KN/m^3 is the specific weight of water, and h_n is the net head. We remark that the net head is function of discharge and the geometrical properties of the conveyance system (details are given in section 2.2). On the other hand, the total efficiency is the product of the turbine efficiency, n_T, referring to the conversion of kinetic into mechanical energy, and the generator efficiency, n_G, referring to the conversion of mechanical into electrical energy. The latter is practically constant, while the former varies with discharge and head (see section 3.3).

For convenience, the minimum operational discharge is typically expressed as a portion, θ, of the maximum one (e.g., Yildiz and Vrugt, 2018), i.e.:

$$q_{i,min} = \theta\, q_{i,max} \tag{2}$$

The portion θ depends on the turbine type and may range from 5 to 40%.

Let q be the streamflow arriving at the intake, after subtracting the environmental flow, q_e. In the case of small hydroelectric works, this is a constant value that is enforced to pass over the intake by priority. Typically, this is determined after analyzing the low flow regime of the river and should be ensured with very high reliability.

The flow passing from the first turbine is given by:

$$q_{T1} = \min(q, q_{1,max}) \tag{3}$$

If $q > q_{1,max}$ then the surplus flow passing from the second turbine is:

$$q_{T2} = \min(q - q_{T1}, q_{2,max}) \tag{4}$$

For $q_{Ti} < q_{i,min}$ the turbine is set out of operation, while for $q_{Ti} > q_{i,min}$ the energy produced by each turbine is:

$$E_i = \eta(q_{Ti})\, \gamma\, q_{Ti}\, h_n\, \Delta t \tag{5}$$

where Δt is the time interval of calculations.

In some cases, the operation of SHPPs is interrupted when the inflow reaches a safety value, q_s, in order to protect turbines against erosion. Under this premise, if $q > q_s$, the produced energy is set equal to zero. The value of q_s is usually estimated by means of an extreme flow quantile, depending on local conditions (Hänggi & Weingartner, 2012). A typical value is the river discharge with exceedance probability 2%. This operational constraint mainly involves run-of-river schemes in mountainous areas with high sediment yields, like the Alps, the Andes and the Himalaya. We emphasize that hydro-abrasive erosion is strongly unfavorable, since it affects the turbine efficiency, and increases costs for repairs and replacements (Felix *et al.*, 2021).

2.2 Estimation of net head

The net head, h_n, is calculated as follows:

$$h_n = h_g - h_f - h_L \tag{2}$$

where h_g is the gross head, i.e. the elevation difference from the upstream water level (forebay) to the power station outlet (practically constant), h_f are the friction losses along the penstock, and h_L are the cumulative minor hydraulic losses. For a pipe of length L, diameter D, and roughness ε, the friction losses, which are the main component of total hydraulic losses, are given by:

$$h_{\mathrm{f}} = f(D, \varepsilon, q)\, L \frac{8\, q^2}{\pi g D^5} \tag{6}$$

where f is a dimensionless friction factor. The above formula is strongly nonlinear, thus in the literature many researchers have proposed simplified expressions to calculate f (e.g. Koutsoyiannis, 2008).

On the other hand, local, also referred to as minor hydraulic losses, are occurring at every change of geometry (transition) and thus change of flow conditions (e.g., flow entrance through the intake, change of diameter, flow split, elbow, etc.). Each individual loss is generally estimated by:

$$h_{\mathrm{L}} = k \frac{v^2}{2g} \tag{7}$$

where k is a dimensionless coefficient, depending on transition geometry, and v is the flow velocity, given by $v = 4q/\pi D^2$.

2.3 Estimation of efficiency

Large hydroelectric reservoirs allow for controlling outflows, thus their turbines are normally working in the nominal flow, which maximizes efficiency (Andreas Efstratiadis *et al.*, 2021). In contrast, the turbines of SHPPs are operating under a wide range of flow conditions, where η is strongly varying across the feasible flow range (q_{min}, q_{max}).

As shown in Figure 1, for specific turbine dimensions (e.g., diameter runner), its efficiency, n_T, is usually expressed by means of nomographs, as percentage of the rated flow, q_T/q_r, where q_r refers to the nominal discharge of the turbines, ensuring the best efficiency (typically, this coincidence the maximum flow capacity, thus $q_r = q_{max}$). These originate from reduced scale models, by making the hypothesis of dynamical, geometrical, and kinematical similarity between the model and the prototype. Although empirical corrections are employed to better reflect the prototype performance, the actual efficiency is as highly uncertain input to flow-energy conversion (Hidalgo *et al.*, 2012), since it also depends on constructive and operational characteristics of the power plant, as well as changes due to deterioration, damage and aging of equipment over time (Paish, 2002), mainly due to erosion effects (Felix *et al.*, 2016).

For modelling purposes (e.g., simulation, scheduling, design optimization), analytical formulas are generally preferred instead of nomographs. These are typically expressed either as piecewise linear (Basso & Botter, 2012, Skjelbred & Kong, 2019) or polynomial equations (Diniz *et al.*, 2007, Roy, 2005). Here, we introduce an alternative expression for turbine efficiency, i.e.:

$$n_T = n_{min} + \left(1 - \left(1 - \left(\frac{\frac{q}{q_{max}} - \theta}{1 - \theta}\right)^a\right)^b\right)(n_{max} - n_{min}) \tag{8}$$

where n_{min} and n_{max} are the upper and lower efficiency values within the feasible flow range (q_{min}, q_{max}), and a and b are shape parameters. The above relationship is more consistent, since it explicitly accounts for the actual technical characteristics of turbines, particularly the ratio θ and the extreme efficiency values, n_{min} and n_{max}. Another advantage is the flexible and parsimonious parameterization, by means of only two shape parameters, in contrast to other literature expressions that require numerous input arguments, without physical sense.

By changing *a, b,* n_{min}, n_{max} we can fit eq. (8) to practically any empirical efficiency curve, thus significantly facilitating calculations. This change is not just about the limits to which the curve fluctuates (n_{min}, n_{max}), but also is concerned about the camber and generally the way this curve reaches n_{max}. Since the nomographs refer to the turbine efficiency, for the extraction of total efficiency we should also account for additional energy losses in the generator and the transformer. Typically, an overall correction is employed, by multiplying the data by a constant value that may range from 0.88 to 0.97.

In the present study, we investigate the performance of two commonly used turbines, namely Francis and Pelton. The Francis turbine belongs to the group of reaction turbines, and use the force exerted by the water to rotate the runner inside the turbine, in a way similar to how the engines of an airplane create trust. Reaction turbines exhibit a rather poor efficiency at low flows despite their relatively high specific speeds. As for the Pelton turbine, it is the main type of impulse machines and its strong advantage over the Francis turbine is the approximately stable efficiency for quite a large range of flows.

3 The inverse problem

In this section we present the methodology for extracting the inflow arriving at the intake of a SHPP without regulation (e.g., due to a storage component), for given energy production, also called the inverse hydroelectricity problem (Sakki, 2020). In the generic case of turbine mixing, the individual production from each turbine is known. Herein we distinguish three possible modes, depending of the associated energy production:

- at least one turbine is in operation;
- both turbines produce their maximum potential energy;
- no energy is produced.

For simplicity, next we discuss the case of a single turbine. The inverse formulation of the flow-energy conversion is next generalized, to embed two major sources of uncertainty, by means of observational errors in energy production data and the uncertainties on the technical characteristics of the system, e.g. the efficiency of turbines.

At the end, we add the environmental flow, q_e, to retrieve the full hydrograph. In a design context, the value of q_e, either constant or seasonally varying, is determined by the national legislation. Here we apply the legal value, considering that the associated constraint is systematically fulfilled. In a real-world operation of SHPPs, this may not be valid, thus introducing another aspect of uncertainty in the inverse problem, which is yet not much important, if compared to other ones.

3.1 Extraction of turbine flows

The computational procedure for the inverse problem of hydroelectricity is summarized in Figure 2. At each time step, we consider a given energy production, E, over a time interval Δt, and solve for the flow that passes through the turbines, q_T, which is calculated by:

$$q_T = \frac{E}{\gamma\, \eta(q_T)\, h_n(q_T)\, \Delta t} \tag{9}$$

Its value can be estimated through an iterative numerical scheme, accounting for nonlinearities induced by efficiency and net head formulas, $\eta(q)$ and $h_n(q)$. Therefore, in contrast to the forward problem, for which we can extract the full time series of power production from a given streamflow sample, the inverse problem is not well-posed, since for a given energy record only part of the corresponding streamflow set can be retrieved directly.

For each time step, it is first necessary to check whether the flow passing through the turbines, q_T, equals the input streamflow, q, which is true only when the energy production, E, is positive and less than its maximum potential value, i.e. $P\,\Delta t$. The following cases arise:

- If $E = 0$ then $q \le q_{min}$ (no energy is produced, since the streamflow arriving at the turbines is less than the minimum operational value) or $q \le q_s$ (in the occasional case of exceeding the safety limit beyond which the turbine operation ceases);
- If $E = P\,\Delta t$ then $q \ge q_{max}$ (the streamflow exceeds the nominal discharge of turbines, and the surplus quantity spills over the weir);
- If $0 < E < P\,\Delta t$ then $q = q_T$.

The first case refers to two extreme operational models of the system, which are easily recognized. In particular, the drop of flow below the minimum operational value, q_{min}, is expected to happen during dry periods. On the other hand, the exceedance of the safety flow limit, q_s, takes place only during large flood events, and can be straightforwardly detected due to a sudden shut-down of energy production.

In the intermediate region, which is expected to cover significant portion of time, we compute the turbine flow for time step t = 1, …, n by using the deterministic inverse formula $q_T = f(E)$, which is expressed in the following recursive form:

$$q_T^{[j]} = \frac{E}{\gamma\, \eta\left(q_T^{[j-1]}\right)\, h_n\left(q_T^{[j-1]}\right) \Delta t} \tag{10}$$

where j is a counter. To run the formula, an initial flow value, $q_T^{[0]}$, is assigned, typically the last known value of the simulated data, q_{t-1}. This iterative scheme usually converges after two or three repetitions. The termination condition for this iterative procedure is expressed in terms of absolute difference, Δq, between two subsequent estimations of the flow value, i.e.:

$$|q_T{}^{[j]} - q_T{}^{[j-1]}| < \Delta q \tag{11}$$

3.2 Extrapolation outside the operational flow limits

The aforementioned methodology is only valid for the flow range between q_{min} and q_{max}. The missing values are estimated by extrapolating the simulated turbine flows outside this range, thus obtaining the upper and lower part of the hydrograph that cannot be extracted by the inverse problem. Two characteristic examples, which are obtained from our proof of concept in the context of section 5, are given in Figure 3. Essential requirement to apply extrapolations is the limited duration of operation outside of the flow limits q_{min} and q_{max}. In an efficiently-designed system, this is by definition ensured, as the turbines are selected in order to operate significant portion of time.

We remind that the maximum discharge that can pass from the turbines is restricted by the power capacity, thus when the system produces its maximum potential energy, we do know that the flow exceeds its nominal discharge, q_{max}. On the contrary, the minimum discharge that can be estimated through the inverse procedure is the lower flow value to produce energy. When the energy production is zero, the flow is under q_{min}, except for the specific case of turbine interruption for safety reasons, which means that the arriving flow is beyond the threshold, q_s, or when the turbines are out of operation for maintenance reasons.

3.2.1 High flows

The flood flows over the discharge capacity of turbines, q_{max}, that arrive at the inlet of a small hydropower plant, as well as the flood duration, are essential elements of its operation, during which the surplus inflow spills over the weir. Their estimation is based on the extrapolation of the rising and falling limb of the flood hydrograph, for a given sequence of known turbine flow values little before and little after the operation of turbines in their maximum capacity, respectively. As illustrated in Figure 4, the proposed extrapolation scheme follows two key principles, i.e. (a) the rising limb after the last known flow value up is linear, and (b) the falling limb is exponentially decreasing downwards to the first known flow value.

Let a time interval of N steps of duration D after time T, during which the turbine produces its maximum potential energy, thus $q_t > q_{max}$ for $t = T + 1, \dots, T + N$. In this respect, the two last known flow values that are extracted from the inverse formula are q_T and q_{T-1}. In order to extrapolate the hydrograph forward, we compute the slope of the linear rising limb, which is:

$$\xi = \frac{q_T - q_{T-1}}{D} \tag{12}$$

Any forward discharge value is calculated by using the relationship:

$$q_t = max(q_{max}, q_{t-1} + \xi\ t)\text{ , for } t = T + 1, \dots, T + N \tag{13}$$

The above formula ensures that all estimated flow values in the rising limb will exceed the nominal flow, q_{max}, otherwise they are manually set equal to q_{max} (as made in the example shown in Figure 3 (a)). The specific case of interruption of turbine operation for safety reasons, is handled in the same manner, by substituting q_{max} by q_s.

As for the falling limb, the extrapolation is employed backwards, following a negative exponential law, based on the well-known linear reservoir approach, which is a simple yet effective model for describing recession phenomena, e.g. low flows through the groundwater zone and flood recessions (Risva *et al.*, 2018). Under this assumption, the discharge after peak flow, q_p, is calculated by:

$$q_t = q_p \exp(-kt) \tag{14}$$

where k is a recession parameter.

Eq. (14) contains two unknown quantities, i.e. the peak flow and the recession parameter. The latter is easily computed by considering the known (more precisely, reconstructed) flow values q_{T+N} and q_{T+N+1} that are by definition lower than q_{max}. Specifically:

$$k = \ln\left(\frac{q_{T+N}}{q_{T+N+1}}\right) \tag{15}$$

The intercept point of the two extrapolations (forward linear and backward exponential) is the estimator of the peak discharge, which occurs in an intermediate time between two subsequent time indices. For the determination of peak flow, we introduce an additional time interval parameter, τ_p, between q_T and q_p, and next we solve the nonlinear system:

$$q_p = q_T + \xi\ \tau_p \tag{16}$$

$$q_{T+N} = q_p \exp\left[-k\left(T_N - \tau_p\right)\right] \tag{17}$$

Critical issue in the above procedure is the estimation of the recession rate k, which is a highly uncertain parameter. In fact, data analysis worldwide highlights that k exhibits significant variability across different flood events and discharge rates, thus confirming the stochastic nature of the recession process (Fiorotto & Caroni, 2013, Krakauer & Temimi, 2011, Tallaksen, 1995). This variability is also evident in the examples shown in Figure 2. The proposed method for retrieving inflows also allows for establishing representative patterns for hydrograph recession, for infilling missing data, and also for assessing the underlying uncertainty, if treating the recession parameter as a random quantity.

3.2.2 Low flows

Similar to the estimation of high flows, it is necessary to represent the period of low flows. This extrapolation is very important for a small hydropower plant, because the duration and the frequency of these periods may be crucial for the scheduling of the operation of power plant and the prediction of its performance. For instance, if these periods are extended or they happen too often, then the plant is not efficient. Due to all uncertainties, which are also mentioned before, it is possible that a power plant will not be as efficient as hypothesized in its design.

As shown in Figure 3 (c) and (d), the hydrograph extrapolation for low flows follows the same idea with the extrapolation of high ones. The recognition of low flow periods is straightforward, since during this period the power production is zero. The estimation is based on the forward extrapolation of the falling limb and the backward of the rising one, using the same assumptions with high flows, i.e. the rising limb is linear the falling exponential. It is worthy commendable that if the any estimated discharge value exceeds the minimum flow, it is manually set equal to q_{min}.

3.3 The inverse problem of hydroelectricity in stochastic setting

In a real-world study, the flows that are retrieved from energy data will deviate from the actual ones, due to errors and uncertainties that appear in all components of the flow-energy transformation procedure. All these are transferred as model errors (also referred to as residuals), i.e. deviations of simulated from actual flow data.

Herein we provide two alternative means to quantify the uncertainty of extracted inflows. When observed inflow data is missing, to allow estimating the actual statistical and stochastic properties of residuals, the uncertainty of inflows is artificially assigned, by expressing the key uncertain components of the hydropower system as random variables. This requires employing a priori hypotheses about the probabilistic regime of the associated variables, which is essentially subject of experience.

On the other hand, when actual inflow data are available, we can directly express the total uncertainty of the inverse modeling procedure, by extracting the streamflows, computing the residuals and estimating their probabilistic and stochastic regime a posteriori. This option is applicable even when the hydrological data are fragmented, provided that the associated statistical information for the model residuals is representative. This allows for infilling the missing inflow data by accounting for the actual model uncertainty, without needing manual assumptions, as made in the a priori approach.

3.3.1 A priori assignment of uncertainty to flow-energy conversions under missing inflow data

An apparent source of uncertainty refers to the output quantity per se, i.e. energy data. Potential reasons are measurement errors (which are yet not so much important), as well as errors due to the large extent of associated information, quite often requiring post-processing and clearance. The uncertain energy production is easily expressed by adding an error term, ΔE_t, to the measured energy E_t, as follows:

$$E_t^* = E_t + \Delta E_t \tag{18}$$

The error term is given in statistical terms, by considering a suitable distribution function. If the error is non-systematic, we can simply assign a white noise model. On the other hand, if we know that the power production is over- or under-estimated, it is desirable to apply a skewed error (with negative or positive skewness, respectively).

However, the major facet of uncertainty in SHPP systems involves the actual performance of turbines. On the one hand, the theoretical efficiency curves, as provided by manufacturers and used in design studies, often do not fit well to the real-world operation of turbines. For this reason, the design nomographs may deviate significantly from the actual efficiency in the field, which affects a wide range of applications, including performance assessment, real-time operation and power predictions.

On the other hand, the turbine efficiency drops significantly due to aging and malfunction effects. For, the experience so far reports quite many problems in small hydroelectric works, since after only few years of operation, turbines can show significantly reduced performance due to cavitation, erosion, fatigue and material defects. Interestingly, the deviation from the theoretical efficiency curve is not uniform. As mentioned by Abbas & Kumar (2019), the uncertainty on efficiency measurements around the best efficiency point has been found to be the minimum one, with respect to other parts of the efficiency curve.

In order to evaluate the impacts of possible sources of uncertainty on the system's efficiency we use the proposed analytical formula (8). The parametric expression allows for quantifying such uncertainties by assigning proper statistical distributions to the system's properties, i.e. the minimum and maximum efficiency, n_{min} and n_{max}, as well as the shape parameters, a and b. The quantification of parameter uncertainty can also account for the aforementioned aging effects, provided that the associated error is expressed through non-Gaussian statistical models.

In this respect, we can generate a large enough number of scenarios, combining uncertain energy production data and uncertain efficiency curves, and solve the inverse problem in a Monte Carlo chain to obtain multiple realizations of inflows under uncertainty. The latter are used to extract typical uncertainty metrics of the modelled flows, such as expected values and confidence intervals.

3.3.2 A posteriori expression of uncertainty based on statistical analysis of inverse model residuals

First, we solve the problem as deterministic, by estimating the flows that pass from the turbines through the iterative numerical scheme, using the given energy production data. We remind that this only involves part of the full hydrograph between the minimum and maximum operational discharge of the system; the full streamflow data also comprises higher and lower values, which are estimated through the extrapolation scheme of section 3.2. The next step is the comparison with the observed streamflow data. Following this, the residuals are represented through an error function, by extracting their statistical characteristics and next fitting a suitable distribution. Under this premise, we finally generate many synthetic error realizations and the associated ensembles of inflows. In this respect, the retrieved and/or the extrapolated streamflow is expressed in stochastic terms, as the unique means for consistent quantification of uncertainty, thus allowing to express the overall uncertainties of the inverse transformation in typical statistical terms (e.g., marginal statistics and confidence intervals).

In the proposed framework, the model residuals are handled as random variables that follow a specific distribution and have a specific autocorrelation structure. Although an ideal model error should follow the white noise properties, thus being homoscedastic and uncorrelated both in "space" (correlation with the parent process, e.g., flow) and time, in the real world we cannot avoid the existence of dependencies. In this respect, for the generic case we should represent the residuals through a *stochastic model*, not simply a statistical one (A. Efstratiadis *et al.*, 2015).

The common expression for model residuals between a simulated and an observed process (in the particular case, streamflow) is:

$$w_t = q_{sim,t} - q_{obs,t} \tag{19}$$

The formulation of the stochastic model for residuals implies the computation of their marginal statistical characteristics and dependence properties, such as the mean, variance, skewness, autocorrelation, and the cross-correlation between the observed flows $q_{obs,t}$ and the error data w_t. If the autocorrelations are large, it is suggested to use a stochastic model that allows to also describe the dependence structure of the error process (Tsoukalas *et al.*, 2020).

In our analyses, the representation and synthesis of model residuals w_t is employed through a first order autoregressive (Markov) model, AR(1), i.e.:

$$w_t = \rho\, w_{t-1} + z_t \tag{20}$$

where w_t is the error process, with mean μ, standard deviation σ, skewness γ, and lag-1 autocorrelation coefficient ρ; ρ is the first order autoregression coefficient; and z_t is an i.i.d. process with mean μ_z, standard deviation σ_z and skewness coefficient γ_z. The statistical characteristics of z_t are related with those of w_t by:

$$\mu_z = \mu_w\,(1-\rho) \tag{21}$$

$$\sigma_z = \sigma_w \sqrt{1-\rho^2} \tag{22}$$

$$\gamma_z = \gamma_w\, \frac{1-\rho^3}{(1-\rho^2)^{3/2}} \tag{23}$$

The next step is the generation of m synthetic error realizations ("ensembles"), by using the Gamma distribution. The Gamma distribution can be parameterized in terms of a shape parameter κ and an inverse scale parameter λ, called a rate parameter. The corresponding probability density function (PDF) is:

$$f(x) = \frac{\lambda^{\kappa}}{\Gamma(\kappa)}(x-c)^{k-1}\, e^{-\lambda(x-c)}, x \geq 0 \tag{24}$$

The stochastic model runs to generate m sets of synthetic error realizations $w_{j,t}$ (also referred to as *ensembles*) for the same time horizon n with the observed flow data. The number of ensembles should be large enough to allow for describing the model uncertainty as much as more accurately. These are next used to get the associated discharge scenarios (turbine flows) for each ensemble $j = 1, \ldots, m$ by employing the inverse transformation:

$$q_{T,j,t} = f(P_t) + w_{j,t} \tag{25}$$

The quantification of uncertainty for each time step t is employed by estimating the statistical characteristics of the corresponding sample of synthetic flow values $q_{T,j,t}$. The latter are empirically expressed in terms of quantiles, e.g. median. In this respect, we also provide confidence intervals based on empirical estimation of two characteristic quantiles (low, high) for each time step t, for a given confidence level (the latter describes the uncertainty of a sampling method). It is necessary to select a confidence level γ, such as 90, 95, or 99%; but any percentage can be used, depending on the size of sample, i.e. the number of ensembles, m. In this respect, for each time step we create the upper and lower limits of the confidence interval using the following functions:

$$q_{upper} = q_{(1+\gamma)/2} \tag{26}$$

$$q_{lower} = q_{(1-\gamma)/2} \tag{27}$$

where the subscript denotes the quantile of simulated flow values for each specific time step. For instance, for $m = 100$ and $\gamma = 90\%$, the confidence limits are captured by the 5th larger and 5th smaller flow value, and they are generally not symmetric with respect to the median.

4 Case study

In order to put in practice the inverse conversion problem and the extrapolation of high and low flows, we formulate a theoretical example involving a small hydropower plant under study, located at Evinos river basin, Western Greece. The plant contains a single turbine of 10.8 MW power capacity and its operation is tested by using daily inflows over a ten-year period. In order to assess the methodology under different efficiency curves, two alternative turbine types are considered, i.e., Pelton or Francis, operating at low flow limits of 10%. Their efficiency as function of rated discharge is expressed by applying eq. (8), using the optimized parameters of Figure 1.

For the estimation of the characteristic flow limits of the system, we assume a constant net head $H_n = 260\, m$, and an average total efficiency $\eta = 0.85$. Thus, for a power capacity of 10.8 MW, we get a maximum operational discharge of approximately 5.0 m^3/s. Consequently, the minimum discharge to produce energy is 0.5 m^3/s, for both turbines.

In order to provide a realistic proof of concept of the inverse problem, we initially run the forward one, and extract a time series of “actual” power production, by considering that both the inflows and the system characteristics (i.e., efficiency curves), are known. Next, we assign artificial errors to two crucial elements of the hydroelectric system, namely the power production data and the efficiency, to represent a real-world environment, where the extraction of streamflow from energy is subject to multiple uncertainties.

In this study, the two aforementioned error expressions, which can be characterized as observational and parametric, are modeled separately. In particular, the observation errors are formalized as random perturbations to the power generation data, by assigning an additive error term that follows either a normal or a skewed (Generalized Gamma) distribution. On the other hand, the extraction of discharge data under parameter uncertainty is made by means of a set of 100 randomly generated efficiency curves around the "actual" ones (Pelton or Francis). In the first setting, the uncertain discharge data are represented in stochastic terms, i.e. by employing the AR(1) model to residuals, while in the second setting the ensembles are directly obtained by solving the inverse problem for each equifinal efficiency curve (term "equifinal" is applied to denote that all curves are equivalently possible to be the true ones).

4.1 Uncertain energy observations

The uncertain energy production is represented through eq. (18), where the error term, ΔE_t, is expressed by means of unbiased noise, thus $\mu_e = 0$. We investigate two alternative distributions with three settings each one, to describe artificial errors, i.e. (a) Normal $N(\mu_e, \sigma_e)$, with standard deviation expressed as percentage of the standard deviation of simulated power production, $\hat{s}_P$, and (b) three-parameter Gamma with standard deviation $\sigma_e = 0.01\hat{s}_P$ and skewness γ_e.

The results for the different error settings are summarized in Tables 1 and 2, for the Normal and Gamma-distributed errors, respectively. Interestingly, the two turbine types exhibit quite different statistical behavior, in terms of error properties. In general, the extraction of flows by considering the Francis turbine results to more uncertain estimations. This is due to the form of its efficiency curve, which exhibits larger variations against flows, and the small flow range that can be captured by this turbine type. As shown in Figure 5 (operation of the system within the flow range of turbines) and Figure 6 (characteristic cases of extrapolation outside the flow limits), the proposed setting allows for expressing different ranges of uncertainty and assessing the impacts of power measurement errors to streamflow estimations, as extracted from the inverse approach.

4.2 Uncertain efficiency curves

In this problem, we first extracted the optimized parametric curve for the Francis case, by solving the calibration problem with given inflow and power data, as provided by the forward problem and by considering the empirical curve. The derived parameter values were $n_{min} = 0.33$, $n_{max} = 0.93$, $a = 0.80$, and $b = 3.75$. Next, we generated 100 random curves around the "true" one, by sampling from the parameter distributions that are given in Table 3. In Figure 7 we depict the full range of synthetic curves around the true efficiency. Interestingly, these are not uniformly distributed, in order to represent the fact that the actual efficiency is expected to be lower than the ideal nomograph provided by the manufacturer. As shown in Figure 8, the uncertainty on efficiency, which is key internal component of the flow-energy conversion, is directly reflected as uncertainty on the simulated flows.

5 Conclusions

The reproduction of streamflow information by taking advantage of power production data, here named as the inverse problem of hydroelectricity, is a challenging task, not only due to the complexities of the numerical problem per se, but also because of the multiple uncertainties across the water-energy conversion cycle. In this research, we investigate both the external uncertainties, by means of observational error in power data, and the internal ones, highlighting on the key issue of turbine efficiency.

In this vein, we provide a generic stochastic simulation framework to obtain inflow time series, also including empirical hydrological approaches to infill missing data outside the range of operation of turbines. This approach allows for quantifying the overall uncertainties that are embedded in the aforementioned reverse transformation in typical statistical terms (e.g., marginal statistics and confidence intervals).

We highlight that the proposed methodology is applicable for the "normal" operation of SHPPs, where the flow passing through the turbines is determined by the upstream inflow and the discharge capacity limits, thus the power production is scaled with flow (which means that the production is not curtailed for non-technical reasons, e.g., energy market constraints). The particular case of zero production for safety reasons (see section 3.1) or when the turbines are under maintenance, refers to occasional time periods, during which the retrieval of inflows becomes highly uncertain. However, if the associated information is available by the manager of the power plant, this can be embedded in the inverse algorithm, to improve flow estimations, e.g., if it is known that q exceeds the safety limit q_s.

Key novelty of our research is the development of a generic parametric formula for turbine efficiency, that can fit to a wide range of empirical curves. This allows for expressing uncertainties by means of probability distribution functions of the associated parameters. This expression may also be useful in the case of hydroelectric systems with missing technical data, in which the actual efficiency curve can be approximated through calibration.

The extraction of streamflow time series at the intake of small hydroelectric plants through the proposed methodology has a twofold value. On the one hand, it contributes to the augmentation of hydrological information in ungauged river basins, which is of key importance due to the lack of hydrometric data and the degradation of monitoring infrastructures worldwide. In particular, the extraction of streamflow values outside of the operation flow limits of turbines is of significant importance for several hydrological objectives, such as the analysis of flood events and of the dry-period regime. Even when the flow systematically remains above q_{max} or below q_{min}, thus the full hydrograph cannot be extracted through the proposed extrapolation approach (which is valid for relatively small durations), a macroscopic information is nevertheless obtained, at least in terms of temporal data.

On the other hand, the knowledge of the running flow conditions is valuable in the context of short-term energy scheduling, where the prediction of energy can be better formalised as a flow prediction problem (Drakaki et al., 2021). In this formulation we can first implement the inverse approach to extract the recent flow sequence, next employ a short-term forecasting scheme to obtain future flow ensembles and finally run the forward model to transform them in energy terms. Results on ongoing research will be reported in due course.

Acknowledgements

We are grateful to the Associate Editor, Dr. Flavia Tauro, who coordinated the review procedure, and the two anonymous reviewers for their fruitful comments and suggestions that helped us to improve significantly our article.

References

Abbas, A. & Kumar, A. (2019) Evaluation of uncertainty in flow and performance parameters in Francis turbine test rig. *Flow Meas. Instrum.* **65**, 297–308. doi:10.1016/j.flowmeasinst.2019.01.009

Anagnostopoulos, J. S. & Papantonis, D. E. (2007) Optimal sizing of a run-of-river small hydropower plant. *Energy Convers. Manag.* **48**(10), 2663–2670. doi:10.1016/j.enconman.2007.04.016

Avanzi, F., Maurer, T., Glaser, S. D., Bales, R. C. & Conklin, M. H. (2020) Information content of spatially distributed ground-based measurements for hydrologic-parameter calibration in mixed rain-snow mountain headwaters. *J. Hydrol.* **582**, 124478. doi:10.1016/j.jhydrol.2019.124478

Avellaneda, P. M., Ficklin, D. L., Lowry, C. S., Knouft, J. H. & Hall, D. M. (2020) Improving Hydrological Models With the Assimilation of Crowdsourced Data. *Water Resour. Res.* **56**(5). doi:10.1029/2019WR026325

Basso, S. & Botter, G. (2012) Streamflow variability and optimal capacity of run-of-river hydropower plants. *Water Resour. Res.* **48**(10), 2012WR012017. doi:10.1029/2012WR012017

Blöschl, G., Bierkens, M. F. P., Chambel, A., Cudennec, C., Destouni, G., Fiori, A., Kirchner, J. W., et al. (2019) Twenty-three unsolved problems in hydrology (UPH) – a community perspective. *Hydrol. Sci. J.* **64**(10), 1141–1158. doi:10.1080/02626667.2019.1620507

Diniz, A. L., Esteves, P. P. I. & Sagastizabal, C. A. (2007) A Mathematical Model for the Efficiency Curves of Hydroelectric units. *2007 IEEE Power Eng. Soc. Gen. Meet.*, 1–7. IEEE. doi:10.1109/PES.2007.385632

Dixon, H., Sandström, S., Cudennec, C., Lins, H. F., Abrate, T., Bérod, D., Chernov, I., et al. (2020) Intergovernmental cooperation for hydrometry – what, why and how? *Hydrol. Sci. J.* 1–15. doi:10.1080/02626667.2020.1764569

Efstratiadis, A., Nalbantis, I. & Koutsoyiannis, D. (2015) Hydrological modelling of temporally-varying catchments: facets of change and the value of information. *Hydrol. Sci. J.* **60**(7–8). doi:10.1080/02626667.2014.982123

Efstratiadis, A., Tegos, A., Varveris, A. & Koutsoyiannis, D. (2014) Assessment of environmental flows under limited data availability: Case study of the Acheloos River, Greece. *Hydrol. Sci. J.* **59**(3–4). doi:10.1080/02626667.2013.804625

Efstratiadis, Andreas, Tsoukalas, I. & Koutsoyiannis, D. (2021) Generalized storage-reliability-yield framework for hydroelectric reservoirs. *Hydrol. Sci. J.* 02626667.2021.1886299. doi:10.1080/02626667.2021.1886299

Fekete, B. M., Robarts, R. D., Kumagai, M., Nachtnebel, H.-P., Odada, E. & Zhulidov, A. V. (2015) Time for in situ renaissance. *Science (80-.).* **349**(6249), 685–686. doi:10.1126/science.aac7358

Felix, D., Abgottspon, A., Albayrak, I. & Boes, R. M. (2021) Temporary shutdowns of the high-head run-of-river HPP Fieschertal to prevent excessive turbine erosion during floods. *IOP Conf. Ser. Earth Environ. Sci.* **774**(1), 012029. doi:10.1088/1755-1315/774/1/012029

Felix, D., Albayrak, I., Abgottspon, A. & Boes, R. M. (2016) Hydro-abrasive erosion of hydraulic turbines caused by sediment - a century of research and development. *IOP Conf. Ser. Earth Environ. Sci.* **49**, 122001. doi:10.1088/1755-1315/49/12/122001

Fiorotto, V. & Caroni, E. (2013) A new approach to master recession curve analysis. *Hydrol. Sci. J.* **58**(5), 966–975. doi:10.1080/02626667.2013.788248

Hänggi, P. & Weingartner, R. (2012) Variations in Discharge Volumes for Hydropower Generation in Switzerland. *Water Resour. Manag.* **26**(5), 1231–1252. doi:10.1007/s11269-011-9956-1

Hannah, D. M., Demuth, S., Lanen, H. A. J. van, Looser, U., Prudhomme, C., Rees, G., Stahl, K., et al. (2011) Large-scale river flow archives: importance, current status and future needs. *Hydrol. Process.* **25**(7), 1191–1200. doi:10.1002/hyp.7794

Hidalgo, I. G., Fontane, D. G., Arabi, M., Lopes, J. E. G., Andrade, J. G. P. & Ribeiro, L. C. L. J. (2012) Evaluation of Optimization Algorithms to Adjust Efficiency Curves for Hydroelectric Generating Units. *J. Energy Eng.* **138**(4), 172–178. doi:10.1061/(ASCE)EY.1943-7897.0000074

Kerkez, B., Glaser, S. D., Bales, R. C. & Meadows, M. W. (2012) Design and performance of a wireless sensor network for catchment-scale snow and soil moisture measurements. *Water Resour. Res.* **48**(9), 2011WR011214. doi:10.1029/2011WR011214

Kittel, C. M. M., Jiang, L., Tøttrup, C. & Bauer-Gottwein, P. (2021) Sentinel-3 radar altimetry for river monitoring – a catchment-scale evaluation of satellite water surface elevation from Sentinel-3A and Sentinel-3B. *Hydrol. Earth Syst. Sci.* **25**(1), 333–357. doi:10.5194/hess-25-333-2021

Koutsoyiannis, D. (2008) A power-law approximation of the turbulent flow friction factor useful for the design and simulation of urban water networks. *Urban Water J.* **5**(2), 107–115. doi:10.1080/15730620701712325

Krakauer, N. Y. & Temimi, M. (2011) Stream recession curves and storage variability in small watersheds. *Hydrol. Earth Syst. Sci.* **15**(7), 2377–2389. doi:10.5194/hess-15-

2377-2011

Paish, O. (2002) Small hydro power: technology and current status. *Renew. Sustain. Energy Rev.* **6**(6), 537–556. doi:10.1016/S1364-0321(02)00006-0

Papantonis, D. E. (2008) *Small Hydroelectric Works*. Athens: Symeon Editions.

Risva, K., Nikolopoulos, D., Efstratiadis, A. & Nalbantis, I. (2018) A Framework for Dry Period Low Flow Forecasting in Mediterranean Streams. *Water Resour. Manag.* **32**(15), 4911–4932. doi:10.1007/s11269-018-2060-z

Roy, S. (2005) Optimal Planning of Generating Units Over Micro-Hydro Resources Within a Catchment Area. *IEEE Trans. Energy Convers.* **20**(1), 231–236. doi:10.1109/TEC.2004.842360

Sakki, G.-K. (2020) *Disentangling flow-energy transformations for small hydropower plants: from reverse engineering to uncertainty assessment and calibration*. National Technical University of Athens. Retrieved from https://www.itia.ntua.gr/2053/

Skjelbred, H. I. & Kong, J. (2019) A comparison of linear interpolation and spline interpolation for turbine efficiency curves in short-term hydropower scheduling problems. *IOP Conf. Ser. Earth Environ. Sci.* **240**, 042011. doi:10.1088/1755-1315/240/4/042011

Tallaksen, L. M. (1995) A review of baseflow recession analysis. *J. Hydrol.* **165**(1–4), 349–370. doi:10.1016/0022-1694(94)02540-R

Tsoukalas, I., Kossieris, P. & Makropoulos, C. (2020) Simulation of Non-Gaussian Correlated Random Variables, Stochastic Processes and Random Fields: Introducing the anySim R-Package for Environmental Applications and Beyond. *Water* **12**(6), 1645. doi:10.3390/w12061645

Viglione, A., Borga, M., Balabanis, P. & Blöschl, G. (2010) Barriers to the exchange of hydrometeorological data in Europe: Results from a survey and implications for data policy. *J. Hydrol.* **394**(1–2), 63–77. doi:10.1016/j.jhydrol.2010.03.023

Drakaki, K.-K., Sakki, G.-K., Tsoukalas, I., Kossieris, P., and Efstratiadis, A. (2021) Day-ahead energy production in small hydropower plants: Uncertainty-aware forecasts through effective coupling of knowledge and data. *Adv. Geosci.* (revised version submitted).

Table 1. Statistical characteristics of simulated flow errors for the two turbine types by adding normally distributed artificial errors to power data.

	$\sigma_e = 0.01\hat{s}_P$		$\sigma_e = 0.05\hat{s}_P$		$\sigma_e = 0.10\hat{s}_P$	
	PELTON	**FRANCIS**	**PELTON**	**FRANCIS**	**PELTON**	**FRANCIS**
Mean	0.037	-0.109	0.044	-0.115	0.049	-0.109
St. deviation	0.065	0.201	0.100	0.196	0.139	0.205
Skewness	1.411	1.212	1.968	1.225	1.154	0.921
Autocorrelation	0.619	0.768	0.243	0.736	0.125	0.672
Cross-correlation	0.777	0.312	0.398	0.947	0.310	0.900

Table 2. Statistical characteristics of simulated flow errors for the two turbine types by adding Gamma-distributed artificial errors to power data.

	$\sigma_e = 0.01\hat{s}_P$		$\sigma_e = 0.05\hat{s}_P$		$\sigma_e = 0.10\hat{s}_P$	
	PELTON	**FRANCIS**	**PELTON**	**FRANCIS**	**PELTON**	**FRANCIS**
Mean	0.037	-0.117	0.037	-0.116	0.036	-0.116
St. deviation	0.064	0.179	0.064	0.180	0.060	0.179
Skewness	1.442	0.674	1.174	0.683	0.573	0.680
Autocorrelation	0.600	0.794	0.633	0.795	0.723	0.796
Cross-correlation	0.773	0.968	0.780	0.968	0.862	0.968

Table 3. Statistical characteristics of efficiency parameters.

	Distribution	Remarks	
a	Normal	$\mu = a_{opt}$	$\sigma = 0.05\ \alpha_{opt}$
b	Normal	$\mu = b_{opt}$	$\sigma = 0.05\ b_{opt}$
$\boldsymbol{n_{max}}$	Beta	$a = 2$	$b = 6$
$\boldsymbol{n_{min}}$	Beta	$a = 4$	$b = 2$

Figure captions

Figure 1. Typical turbine efficiency curves that are applied in SHPPs. Continuous lines are nomographs, adapted from Papantonis (2008, p. 231), while dotted lines are derived by fitting the analytical expression (8). The optimized parameters for the three turbine types are demonstrated in the table.

Figure 2. Flowchart of inverse modelling procedure for retrieving the inflows to SHPPs.

Figure 3. Examples of extrapolating high and flow values, when the streamflow exceeds the upper discharge limit (turbine capacity) of 5.0 m^3/s (a, b) or is below the lower operational discharge limit of 0.5 m^3/s (c, d).

Figure 4. Key definitions and concepts for the extrapolation method over of the maximum turbine discharge, q_{max}. Continuous lines represent the part of the hydrograph that is retrieved on the basis of energy production data (section 3.1), while dotted lines represent the extrapolated part up to the estimated peak flow, q_p.

Figure 5. Simulated flows and their uncertainty bounds (90% confidence intervals) for additive error following Normal distribution with $\sigma_e = 0.10\hat{s}_P$ (a) and $\sigma_e = 0.01\hat{s}_P$ (b), by considering a Pelton-type turbine.

Figure 6. Examples of extrapolated flows under uncertainty.

Figure 7. Synthetic efficiency curves around the "true" one.

Figure 8. Simulated flows for the first year of simulation and its uncertainty bounds using randomly generated efficiency curves.

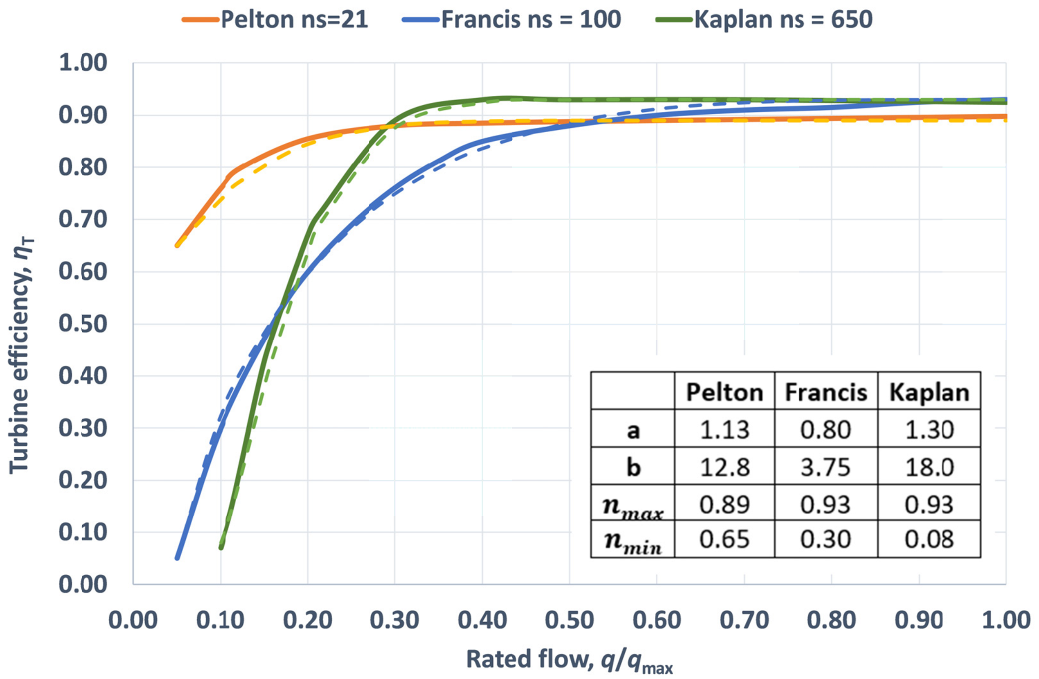

Pelton ns=21
Francis ns = 100
Kaplan ns = 650
Turbine efficiency, η_T
Rated flow, q/q_{max}
1.00
0.90
0.80
0.70
0.60
0.50
0.40
0.30
0.20
0.10
0.00
0.00
0.10
0.20
0.30
0.40
0.50
0.60
0.70
0.80
0.90
1.00
	Pelton	Francis	Kaplan
a	1.13	0.80	1.30
b	12.8	3.75	18.0
n_{max}	0.89	0.93	0.93
n_{min}	0.65	0.30	0.08

Figure 1

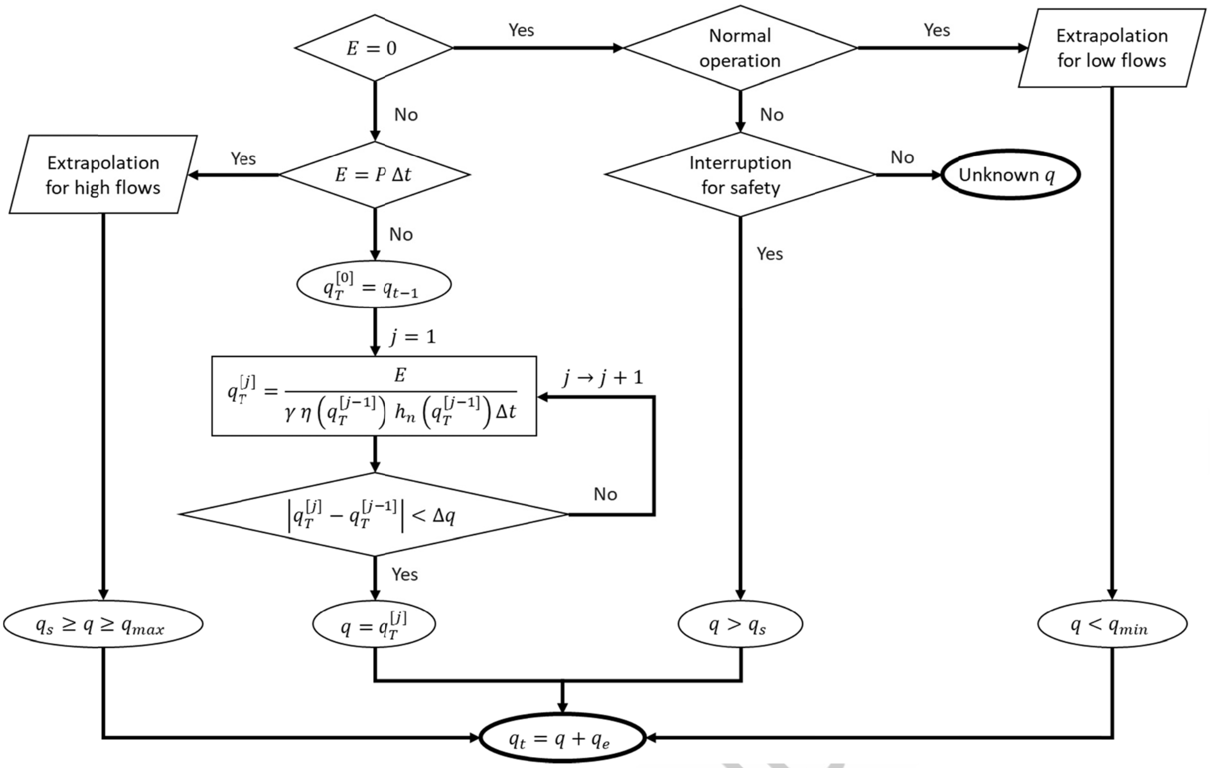
$E = 0$
Yes
No
Normal operation
Yes
No
Extrapolation for low flows
Extrapolation for high flows
Yes
$E = P\,\Delta t$
No
Interruption for safety
No
Unknown q
Yes
$q_T^{[0]} = q_{t-1}$
$j = 1$
$q_T^{[j]} = \frac{E}{\gamma\,\eta\left(q_T^{[j-1]}\right)\,h_n\left(q_T^{[j-1]}\right)\Delta t}$
$j \to j+1$
No
$\left|q_T^{[j]} - q_T^{[j-1]}\right| < \Delta q$
Yes
$q_s \geq q \geq q_{max}$
$q = q_T^{[j]}$
$q > q_s$
$q < q_{min}$
$q_t = q + q_e$

Figure 2

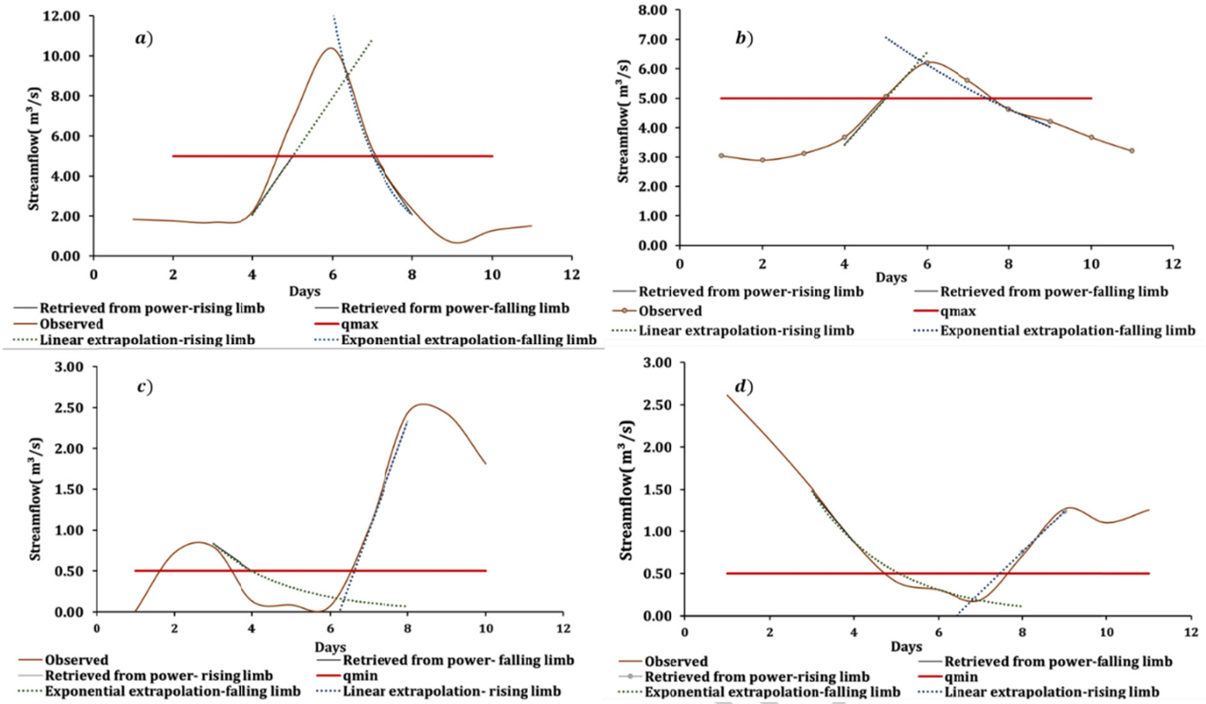
a)
b)
c)
d)
Streamflow(m³/s)
Days
Retrieved from power-rising limb
Retrieved form power-falling limb
Retrieved from power-falling limb
Retrieved from power- rising limb
Retrieved from power- falling limb
Observed
qmax
qmin
Linear extrapolation-rising limb
Exponential extrapolation-falling limb
Linear extrapolation- rising limb

Figure 3

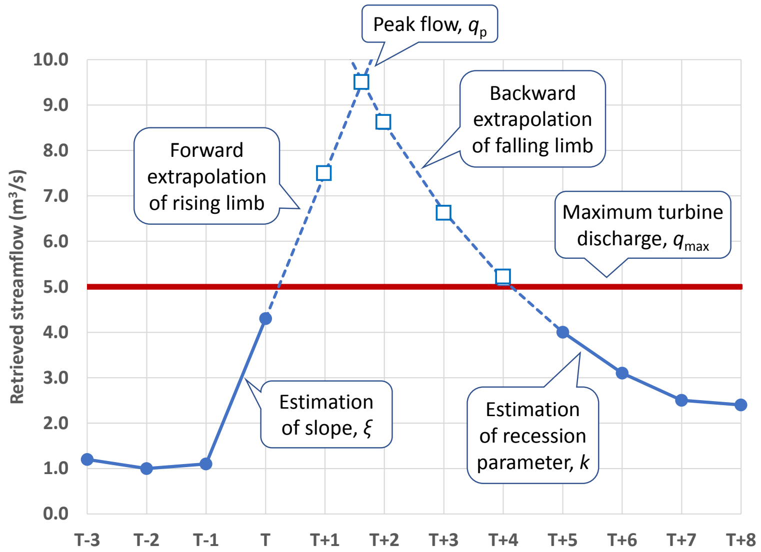

Peak flow, q_p
Backward extrapolation of falling limb
Forward extrapolation of rising limb
Maximum turbine discharge, q_{max}
Estimation of slope, ξ
Estimation of recession parameter, k
Retrieved streamflow (m^3/s)
10.0
9.0
8.0
7.0
6.0
5.0
4.0
3.0
2.0
1.0
0.0
T-3
T-2
T-1
T
T+1
T+2
T+3
T+4
T+5
T+6
T+7
T+8

Figure 4

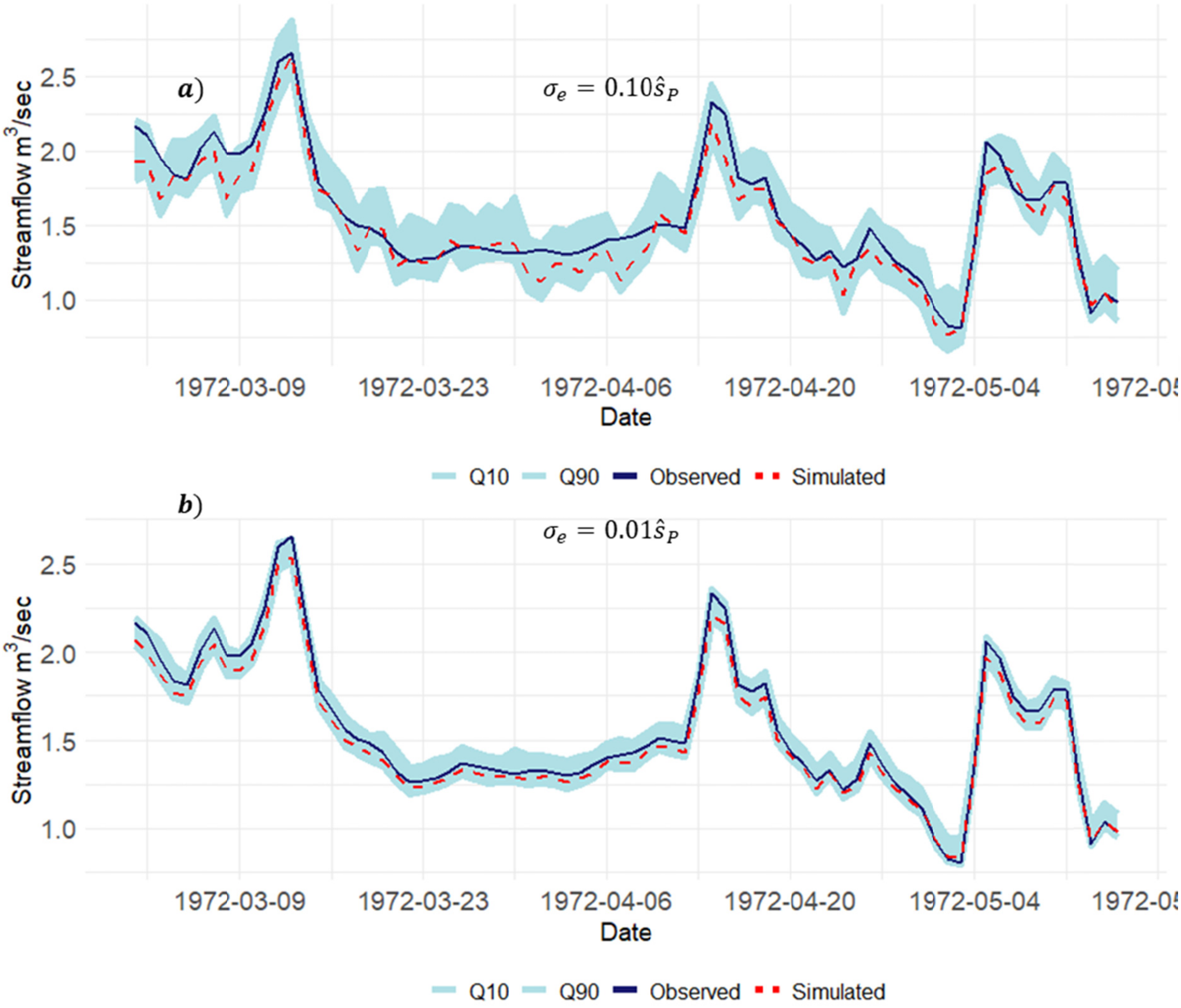
a)
$\sigma_e = 0.10\hat{s}_P$
Streamflow m³/sec
2.5
2.0
1.5
1.0
1972-03-09
1972-03-23
1972-04-06
1972-04-20
1972-05-04
Date
Q10
Q90
Observed
Simulated
b)
$\sigma_e = 0.01\hat{s}_P$
Streamflow m³/sec
2.5
2.0
1.5
1.0
1972-03-09
1972-03-23
1972-04-06
1972-04-20
1972-05-04
Date
Q10
Q90
Observed
Simulated

Figure 5

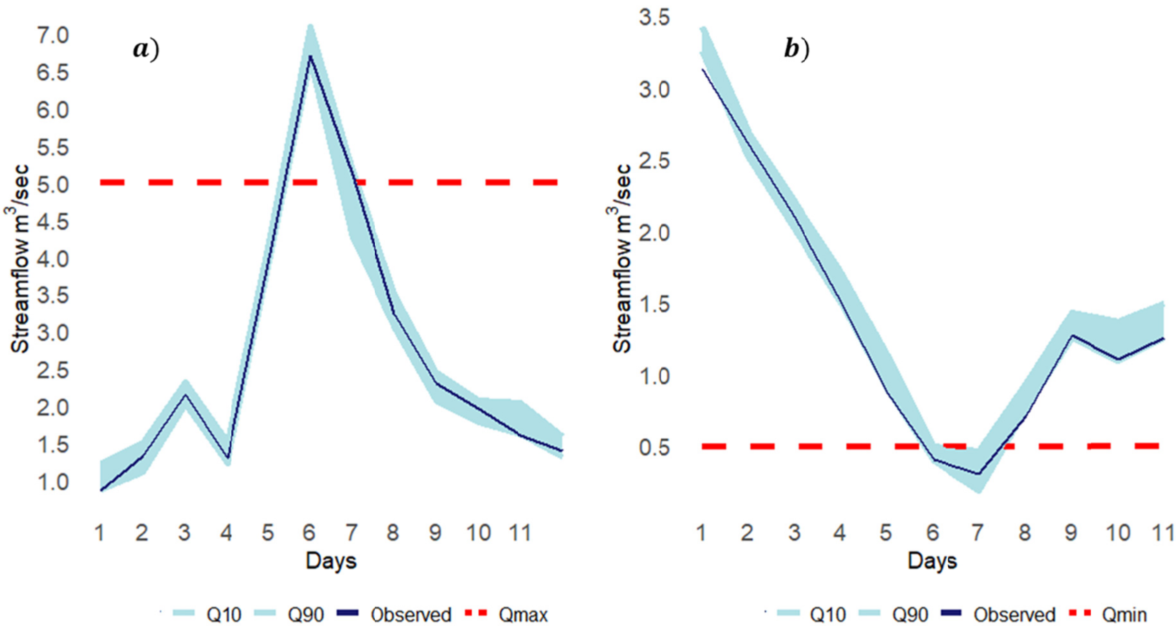

a)
7.0
6.5
6.0
5.5
5.0
4.5
4.0
3.5
3.0
2.5
2.0
1.5
1.0
Streamflow m3/sec
1 2 3 4 5 6 7 8 9 10 11
Days
Q10 Q90 Observed Qmax
b)
3.5
3.0
2.5
2.0
1.5
1.0
0.5
Streamflow m3/sec
1 2 3 4 5 6 7 8 9 10 11
Days
Q10 Q90 Observed Qmin

Figure 6

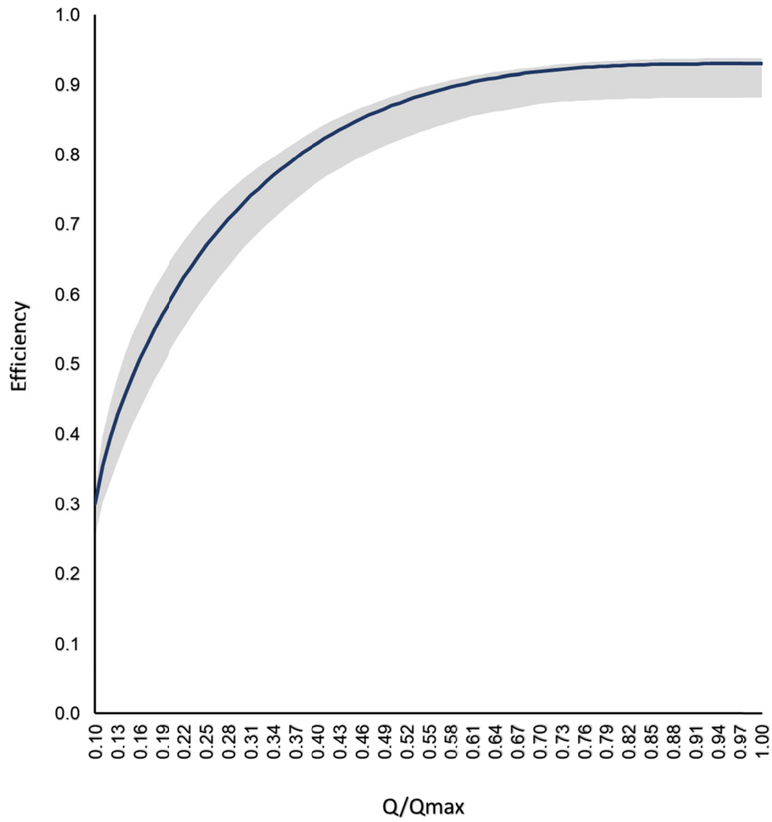
1.0
0.9
0.8
0.7
0.6
0.5
0.4
0.3
0.2
0.1
0.0
Efficiency
0.10 0.13 0.16 0.19 0.22 0.25 0.28 0.31 0.34 0.37 0.40 0.43 0.46 0.49 0.52 0.55 0.58 0.61 0.64 0.67 0.70 0.73 0.76 0.79 0.82 0.85 0.88 0.91 0.94 0.97 1.00
Q/Qmax

Figure 7

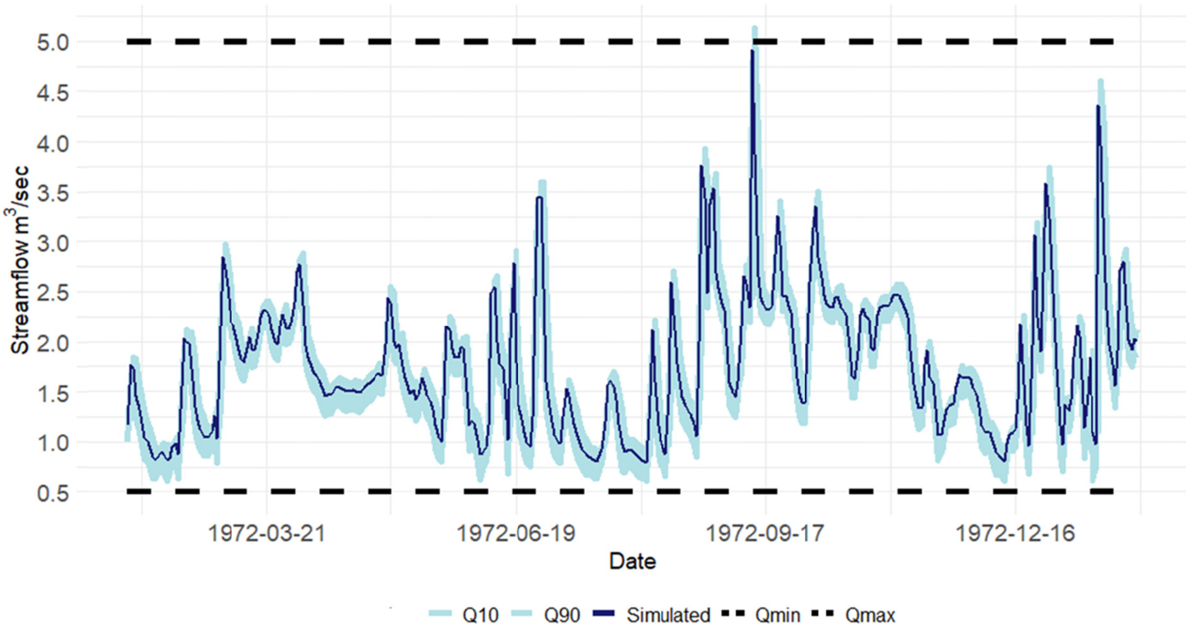

Streamflow m^3/sec
5.0
4.5
4.0
3.5
3.0
2.5
2.0
1.5
1.0
0.5
1972-03-21
1972-06-19
1972-09-17
1972-12-16
Date
Q10
Q90
Simulated
Qmin
Qmax

Figure 8